

Contents lists available at ScienceDirect



journal homepage: www.sciencedirect.com



Effect of solvent polarity on the homogeneity and photophysical properties of MDMO-PPV films: Towards efficient plastic solar cells

S.M. El-Bashir *

Department of Physics & Astronomy, Science College, King Saud University, Riyadh, Saudi Arabia

Department of Physics, Faculty of Science, Benha University, Benha, Egypt



ARTICLE INFO

Article history:

Received 28 May 2017

Accepted 10 September 2017

Available online 18 September 2017

Keywords:

Light emitting polymers

MDMO-PPV

Optical properties

Photoluminescence

ABSTRACT

Thin films of a light emitting polymer Poly[2-methoxy-5-(3',7'-dimethyloctyloxy)-1,4-phenylenevinylene] (MDMO-PPV) were prepared by spin coating on glass substrates using different casting solvents; tetrahydrofuran (THF), chloroform, cyclohexanone, chlorobenzene, xylene, and toluene. The films were characterized by atomic force microscope (AFM), UV-vis absorption and photoluminescence (PL) spectra. The obtained results showed that the casting solvent plays an important role in modifying the film morphology and forming of molecular aggregates. The values of the fluorescence quantum yield and Huang-Rhys factor showed the best interchain interaction and PL properties by increasing solvent polarity. © 2017 The Authors. Production and hosting by Elsevier B.V. on behalf of King Saud University. This is an open access article under the CC BY-NC-ND license (<http://creativecommons.org/licenses/by-nc-nd/4.0/>).

1. Introduction

Conjugated polymers which are known as organic semiconductors have a tremendous interest in the field of development of organic optoelectronic applications such as light emitting diodes (LEDs), field effect transistors (FETs), plastic photovoltaic (PV) cells, lasers, sensors, phototransistors and luminescent solar concentrators (LSCs) (Skotheim, 1997; Sirringhaus et al., 2000; Coakley and McGehee, 2004; McGehee and Heeger, 2000; Gutierrez et al., 2016). The main advantages of conjugated polymers as compared with inorganic or molecular organic materials for optical applications are lower production costs, high flexibility, the possibility of uniformly covering large areas by inexpensive solution processing techniques such as spin coating, drop casting, printing and doctor blade techniques (Kim et al., 2007; Gündüz, 2015; Krebs, 2009). Additionally, there are many ways to fine-tune their optical and electrical properties by varying the composition and structure by their hybridization with inorganic nanomaterials like nanoparticles, nanowires, nanotubes, fullerenes, etc. (Mohan et al., 2017;

Feng et al., 2017; Ren et al., 2010). Moreover, conjugated polymers have been employed as laser gain media for optical amplifier applications with excellent fine tuning in the visible range of the electromagnetic spectrum (Lampert et al., 2017; Frolov et al., 1997; Frolov et al., 2000). Scheme 1. shows the structure of Poly[2-methoxy-5-(3',7'-dimethyloctyloxy)-1,4-phenylenevinylene] (MDMO-PPV) which is a soluble conjugated polymer used in the fabrication of LEDs and as donor material in the fabrication of bulk-heterojunction PV cells (Wienk et al., 2003; van Hal et al., 2003; Rispens et al., 2003; Martens et al., 2003; Mandoc et al., 2007). Many parameters may affect the photophysical properties and surface morphology of the polymer: such as composition, solvent type and the thickness of the active layer (Mohan et al., 2017; Hadzioannou and Van Hutten, 2000; Traiphol et al., 2006). It has been reported that the charge transport is highly anisotropic in conducting polymers, as it is strongly dependent on microstructure, molecular weight, polydispersity which all affect the morphology and carrier mobility in these materials (Österbacka et al., 2000; Brown et al., 2001). As relating the microstructure, morphology, and transport properties in polymeric semiconductors are necessary for the modification of the light emitting properties and the scientific development and successful commercialization of a wide range of electrical and optical applications (Salleo, 2007; Salleo et al., 2004; Rahmanudin and Sivula, 2017). As well, several studies revealed that the morphology of photoactive layers could strongly affect the efficiency and performance of conjugated polymer PV cells (Rahmanudin and Sivula, 2017; van Bavel et al., 2010; Liu et al., 2017).

* Address: Department of Physics & Astronomy, Science College, King Saud University, Riyadh, Saudi Arabia.

E-mail address: elbashireg@yahoo.com

Peer review under responsibility of King Saud University.



Production and hosting by Elsevier

In the present study, we investigated the effect of solvent type on the morphology and spectroscopic properties of spin-coated MDMO-PPV films casted from different solvent types. It has been reported that the casting solvent can strongly affect the film morphology, optical and charge transport properties of conjugated polymers due to various conformations and orientations of the polymeric chain (Mohan et al., 2017; Hadzioannou and Van Huttten, 2000; Traiphop et al., 2006). This study will be helpful to modify the methodology for optimization of the film morphology to enhance the photon trapping efficiency of the polymeric active layer (Park et al., 2009; Liang et al., 2010; Yao et al., 2008).

2. Experimental techniques

2.1. Thin-film preparation

Conjugated polymer MDMO-PPV was obtained from Sigma-Aldrich Co.(USA). It was dissolved with concentration 0.01 g/mL in HPLC grade solvents namely Cyclohexanone, toluene, xylene, chloroform, chlorobenzene and tetrahydrofuran (THF). High-quality microscope slides were cleaned by ultrasonic waves for 10 minutes using acetone and isopropyl alcohol respectively. After that, all the polymer solutions were casted on the glass and spin-coated at 2000 rpm for 40 s. The thicknesses of all MDMO-PPV thin films were measured by Fizeau Fringe experiment and found to be about (200 ± 10 nm).

2.2. Measurements

Fully automated Atomic force microscope, AFM, (NT-MDT SOLVER NEXT, Russia), was used for morphological characterization of MDMO-PPV films. The absorption and specular reflection spectra of the prepared MDMO-PPV thin films were recorded in the wavelength range (300–1000 nm) were obtained using a double beam spectrophotometer model type (JASCO, V-570, UV-VIS-NIR, Japan). Steady-state photoluminescence spectra of the films were recorded in the wavelength range (400–800 nm) using a spectrofluorimeter type model (SCHIMADZU RF-5301 PC, Japan); equipped with a temperature regulator in the range (0–60 °C).

3. Results & discussion

Optical absorption spectra of MDMO-PPV films are shown in Fig. 1. for different solvents at room temperature in the spectral range (350–600 nm). The observed steadiness of the absorption spectra reflects the homogeneity of the polymer molecules in all the prepared films (El-Bashir et al., 2017). It is also noticed that the absorption edge is red shifted by increasing solvent polarity as indicated by the values dipole factor, D , obtained from Koenhen and Smolders (1975) and listed in Table 1. The absorption edge was analyzed for all the investigated films by calculating the absorption coefficient α (Koenhen and Smolders, 1975; Fox, 2002; Pankove, 2012),

$$\alpha = 2.303A/d \quad (1)$$

where A is the absorbance, and d is the film thickness. According to Tauc model (Tauc, 1970), the fundamental absorption coefficient, α , is related to photon energy, E , as the band gap energy can be determined by plotting $(\alpha E)^{1/m}$ versus E where the value of m depending on the nature of the transition. In the current study, the best least square fitting was obtained by taking $m = 1/2$ according to the following relation (Koenhen and Smolders, 1975; Fox, 2002; Pankove, 2012),

$$\alpha E = B(E - E_{gd})^m \quad (2)$$

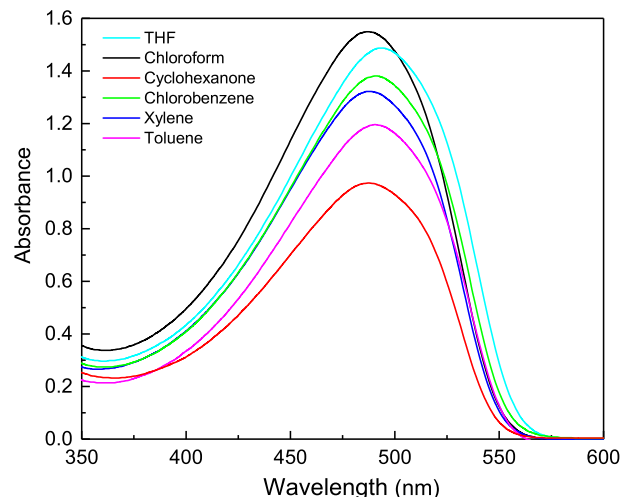


Fig. 1. Optical absorption spectra for MDMO-PPV films casted from different solvents.

where B is constant, and E_{gd} is the energy of the direct and indirect interband transitions respectively (Koenhen and Smolders, 1975; Fox, 2002; Pankove, 2012). According to Eq. (2), the values of E_{gd} were determined for all the investigated MDMO-PPV films as presented by Fig. 2 and listed in Table 1 which shows no significant decrease in the values of E_{gd} is observed. This behavior demonstrates that the solvent type does not strongly alter the bond length and quinoidal character and subsequently the is not decreased (Brédas, 1985; Zheng et al., 2014). The stability of the band structure of MDMO-PPV films by changing the solvent type is well correlated with the photoluminescence (PL) characteristics as will be explained in the following section.

Fig. 3 shows the normalized PL spectra of all the prepared MDMO-PPV films recorded in the spectral range (500–700 nm) at room temperature. The PL peak is composed of three vibronic transitions which are equally spaced in energy and assigned to 0–0, 0–1 and 0–2 transitions, respectively (Nguyen et al., 2001). It was stated that the shape and position of the PL spectra are controlled by (i) the conformational changes of polymeric chains that modify the effective size of the conjugation; (ii) the formation of aggregates and (iii) the interaction with the solvent, producing solvatochromic effects (Quan et al., 2006). The values of the maximum emission wavelength, λ_e , were determined and listed in Table 1; an inspection of the table shows a slight blue shift by increasing the polarity of the solvent. From this study, it is clearly observed that the PL intensity is decreased for aromatic solvents this can be due to the aggregation of MDMO-PPV molecules that happens more readily in aromatic solvents which interact preferentially with the aromatic backbone of the polymer chain. On the other hand, for nonaromatic solvents such as THF are more likely to interact with the side groups of the polymer thus causing the polymer chains to form tight coils and thus reducing the formation of aggregates (Nguyen et al., 2000).

Stokeš shift which is a measure of the spectral overlap between the absorption and PL spectra can be calculated from Lakowicz and Masters (2008),

$$\Delta\lambda_s = \lambda_f - \lambda_a \quad (3)$$

where λ_a and λ_f are the wavelength values of the absorption and PL maxima respectively.

The fluorescence quantum yield, Φ_f , is the most important characteristic of fluorophores as the ratio of the number of the emitted photons to the number absorbed photons (Lakowicz and Masters, 2008),

Table 1

Spectroscopic and optical properties of MDMO-PPV films compared to the dipole factor of the casting solvents D.

Solvent	Cyclohexanone	Toluene	Xylene	Chloroform	Chlorobenzene	THF
D	0	0.31	0.45	1.15	1.54	1.75
λ_a (nm)	481	488	489	490	495	493
λ_c (nm)	550	553	554	553	556	551
$\Delta\lambda_s$ (nm)	69	65	65	63	61	58
$\Phi_f(S)$	0.27	0.3	0.32	0.33	0.36	0.42
HR factor	0.45	0.62	0.73	0.81	0.92	0.95
E_g (eV)	2.296	2.275	2.272	2.266	2.263	2.258
E_a (kJ/mol.)	0.448	0.536	0.617	0.65	0.671	1.169
n	1.97	2.06	2.27	2.34	2.59	2.68
$\eta\%$	87.27	87.4	89.8	90.89	92.26	92.75

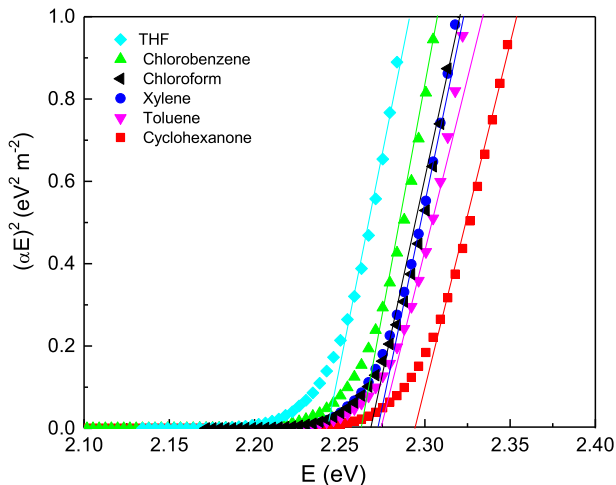


Fig. 2. Direct interband transitions for MDMO-PPV films casted from different solvents.

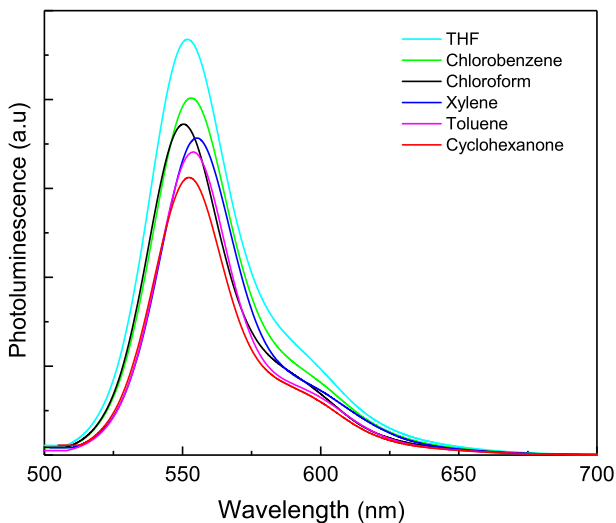


Fig. 3. Fluorescence spectra for MDMO-PPV films casted from different solvents.

$$\Phi_f(s) = \Phi_f(r) \frac{A_r n_s^2}{A_s n_r^2} \frac{\int F_s(\bar{v}) d\bar{v}}{\int F_r(\bar{v}) d\bar{v}} \quad (4)$$

where the integrals over F represent the area of the corrected fluorescence spectrum, A is the absorbance value of the excitation wavelength, and n is the refractive index; the subscripts s and r refer to sample and reference. The values of Φ_f were calculated for MDMO-PPV films taking Rhodamine 6G dissolved in methanol

as the reference fluorophore which showed the best suitable spectral overlap; this solution has a standard value of Φ_f equal to 0.94 (Demas and Crosby, 1971). It is clear from Table 1 shows that the values of Φ_f are increased by increasing the solvent polarity; this increase is accompanied by a decrease in the values of $\Delta\lambda_s$. This behavior is mainly attributed to the formation of higher aggregates which have small values of Φ_f by reducing the solvent polarity. The strength of aggregation depends on the nature of the fluorophore, the polarity of the solvent and the other factors related to the preparation conditions (El-Bashir et al., 2017; Nguyen et al., 1999). Aggregates of polymeric semiconductors exhibit two classes of electronic interactions that occur between chains. The impact of such interactions on the photophysical properties of polymeric films can be understood using the concepts of J- and H-aggregation. In conjugated polymers, the intrachain through-bond interactions lead to the formation of J-aggregates, whereas interchain Coulombic interactions lead to the formation of H-aggregates (Spano and Silva, 2014). The emissive property of conjugated polymer films is controlled by a competition between J-aggregate and H-aggregate interactions in the conjugated π -systems (Baghgar et al., 2014; Lemmer et al., 1995).

The concept of Huang–Rhys factor (HR) correlates with the conformational disorder and indicates the strength of polymer inter-chain interaction (Mohan et al., 2017).

Theoretically, the relative intensity of $0 \rightarrow n$ transition can be calculated from the following equation (Mohan et al., 2017; Quan et al., 2006; Oliveira et al., 2003; Moreno et al., 1992),

$$I_{0-n} = \frac{e^{-HR} (HR)^n}{n!} \quad (5)$$

where n is an index of the vibrational level, and HR is the Huang–Rhys factor, which represents the strength of the electron phonon interaction. Fig. 4. Shows the normalized PL spectra expressed by wavenumber scale and fitted by two Gaussian functions. The relative intensities of the 0–0 and 0–1 vibronic bands were taken from the experimental curves and deconvoluted in two vibronic bands as shown in Fig. 4. using software origin 2017. It is noted that the values of HR values are increased by increasing the dipole factor of the solvent. This means that the greater polymer interchain interaction is obtained for THF and the lower for cyclohexanone as the higher value of HR factor the stronger of polymer interchain interaction and vice versa (Mohan et al., 2017). Moreover, the increase of the conformational disorder produces different types of changes to the spectral profile, such as (i) the broadening of PL spectrum and (ii) shorter conjugation lengths leading to a blue shift of PL spectrum (Quan et al., 2006). This study revealed that decreasing the solvent polarity causes the loosely coiling of the polymer chains that cause the formation of aggregates, on the other hand, tighter coiling of polymeric chains leads to the formation of smaller aggregates (Mohan et al., 2017; Oliveira et al., 2003; Brédas et al., 1996; Basko and Conwell, 2002). Thus, it can be expected that THF-based films have the smallest aggregates due to its high dipole factor

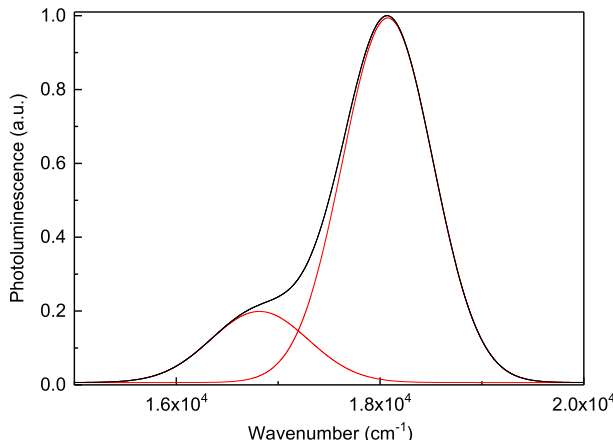


Fig. 4. Normalized fluorescence spectra of MDMO-PPV film casted from chloroform; (The red curves show Gaussian multipeak fitting).

compared to other solvents. These results can be confirmed by AFM study which showed a direct evidence of the dependence of polymer aggregation on solvent polarity. Fig. 5. Shows topographic AFM images clearly showed the larger aggregates for cyclohexanone-based films and smaller aggregates for THF based films. These photos suggest that the degree of homogeneity of polymer chains is increased by increasing the dipole factor of solvents. Based on this discussion, it is clear that the interchain interaction, conjugation length and the coiling of the polymer chains are varied for different solvents. This interchain interaction can either be happened between multiple chromophores of the same polymer chain through coiling/bending back of polymer or between chromophores of different polymer chains. For THF-based films, the polymer chains are not very tightly coiled, so some polymer chains are interacting with each other, and the degree of disorder is decreased (Mohan et al., 2017).

The temperature effect on the PL spectra of MDMO-PPV films was studied in the temperature range (0–60 °C), the normalized PL spectra of THF based MDMO-PPV film is shown in Fig. 6. which represents a representative behavior of the investigated films. It is observed that the PL spectra are blue shifted by increasing the temperature; for the reason that in conjugated polymers, the increase of thermal disorder on heating leads to a decrease in the conjugation length and thereby to a blue-shift and vice versa (Gupta et al., 2002). Additionally; it is observed that as the temperature increases PL intensity decreases to a value I_T of its initial value I_0 , this can be ascribed to the increased phonon assisted relaxation processes as the electronic excitation energy can be dissipated by the vibrational modes existing in the energy levels of the fluorophores (Sumitani et al., 1977). This means that thermally activated processes for fluorescence deactivation from the excited singlet state can be occurred by varying the temperature (El-Bashir et al., 2016). This energy transfer occurs at a rate $K_{ET}(T)$ which is plotted in Fig. 7. according to Arrhenius equation (El-Bashir et al., 2016; Alfassi et al., 1990),

$$K_{ET}(T) = (K_{ET})_{T_\infty} \exp\left(-\frac{E_a}{RT}\right) \quad (6)$$

where I_0 and I_T are the PL intensities at zero and "T" temperatures respectively; "R" is the universal gas constant and E_a is the activation energy of the transfer process; Arrhenius plot of $\ln(I_0/I_T)$ versus $10^3/T$ shows a good linear fit for all the investigated MDMO-PPV films. The calculated values of E_a are listed in Table 1; these values indicate that the thermal stability is improved by increasing the dipole factor of solvent. This can be attributed to the increase of

solvent polarity raised the dipole concentration which requires higher energy to deactivate the photoluminescence process. After shelf-aging of the films for about 24 h; the absorbance is retained to its initial value before heating; this points to the stability of MDMO-PPV films if used in outdoor PV conversion applications at normal atmospheric conditions.

In the transparent range, according to the calculated values of attenuation coefficient k , the refractive index n can be calculated by Fox (2002), El-Bashir (2012),

$$R = (n - 1)^2 / (n + 1)^2 \quad (7)$$

where R is the film reflectance recorded from the specular reflection spectra. Fig. 8. shows the spectral dependence of the refractive index n for all MDMO-PPV films in the wavelength range (300–1000 nm). It is clearly noted that the values of n show normal dispersion according to Cauchy's formula (Fox, 2002; El-Bashir, 2012),

$$\frac{dn}{d\lambda} = -\frac{2B}{\lambda^3} \quad (8)$$

The values of the refractive index, n , are determined in the normal dispersion region (around 1000 nm) and listed in Table 1. It is noted that the refractive index of MDMO-PPV films is increased by increasing the polarity of the solvent; this increase can be explained by the increase of the mean molecular polarizability $\bar{\alpha}$ according to Lorentz-Lorentz equation (Fox, 2002; El-Bashir, 2012),

$$\frac{n^2 - 1}{n^2 + 2} \frac{M_n}{\rho} = \frac{4}{3} \pi N_A \bar{\alpha} \quad (9)$$

where M_n is the molecular weight of the polymer, ρ is the molecular density and N_A is Avogadro's number. This indicates that increasing the solvent dipole factor enlarged the number of atomic refractions due to the increase of the dipole concentration.

The trapping efficiency η , which is the fraction of photons that can be trapped inside the film, was calculated from the refractive index n of the films from the formula (El-Bashir et al., 2016; El-Bashir, 2012; El-Bashir et al., 2014; El-Shaarawy et al., 2007),

$$\eta = \sqrt{1 - \frac{1}{n^2}} \quad (10)$$

The values of η were calculated and listed in Table 1. It is clear that η is increased from 87.27% to 92.75% by increasing the polarity of the solvent. This can be attributed to the increase of the dipole factor that caused the decrease of the critical angle and reduces the fraction of fluorescent photons escaped from the critical cones and accordingly increasing solar energy conversion efficiency (Dienel et al., 2010; Swartz et al., 1977; Batchelder et al., 1981; Debije and Verbunt, 2012). This reveals that THF-based MDMO-PPV films provides the optimum trapping of a larger fraction of photons and consequently improves the optical guiding properties for various applications such as luminescent solar concentrators.

4. Conclusion

From this study, we used spin coating technique for solution casted polymer films; this method is cheap and more accurate to study the optical properties and morphology of MDMO-PPV films. The study showed a slight reduction in the direct band gap, E_{gd} , by increasing the dipole factor of the solvent. The variations in the film morphology and photophysical properties by changing the solvent polarity can be ascribed to the variation in the interchain

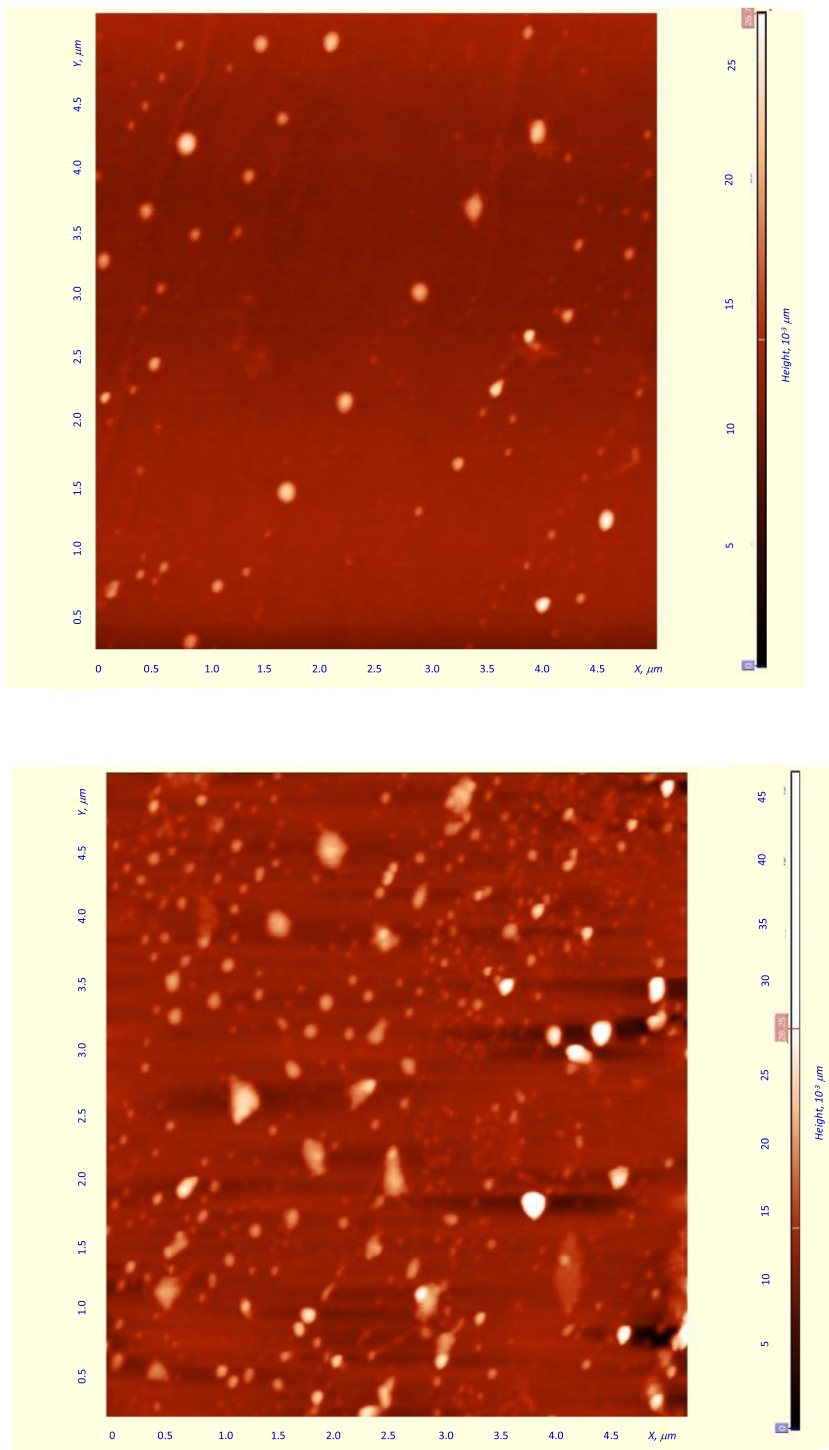


Fig. 5. AFM images for MDMO-PPV films casted from (a) THF and (b) Cyclohexanone; the bright spots indicate polymer aggregates.

interaction which is directly related to the size of the molecular aggregates. The probability of this molecular aggregation is increased by decreasing the polarity of the casting solvent as the nonaromatic solvents such as THF can interact with the side groups of the polymer backbone. This feature caused the polymer chains to form tight coils and minimize the exposure of the backbone thus reducing the formation of aggregates leading to broader PL spectra due to greater conformation disorder. Moreover, a remarkable enhancement of the light guiding properties was attained by

increasing solvent polarity; as the refractive index and photon trapping efficiency is increased. It was found that the optimum film quality and photophysical properties can be achieved by increasing the dipole factor of the casting solvent and the maximum calculated value of photon trapping efficiency, η , was 92.75% and varied as $\eta_{\text{CH}} < \eta_{\text{TOL}} < \eta_{\text{XY}} < \eta_{\text{CF}} < \eta_{\text{CB}} < \eta_{\text{THF}}$. It can be concluded that the proper choice of the casting solvent can strongly affect the film morphology, light emission and optical properties of MDMO-PPV films.

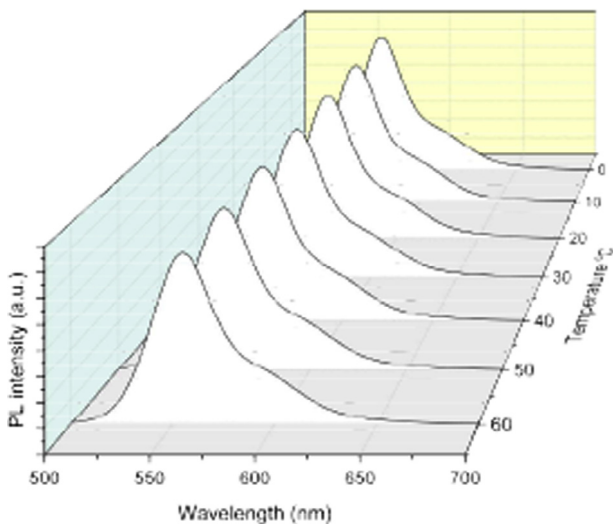


Fig. 6. Temperature dependence of PL intensity for THF-based MDMO-PPV film.

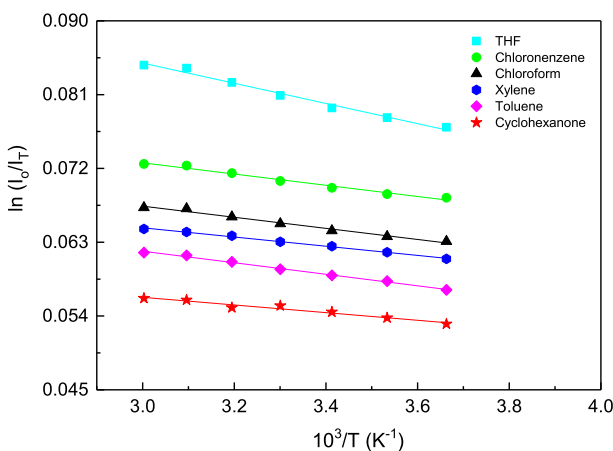


Fig. 7. Relative (I_0/I_r) Fluorescence intensity as a function of temperature for MDMO-PPV films prepared using different solvents.

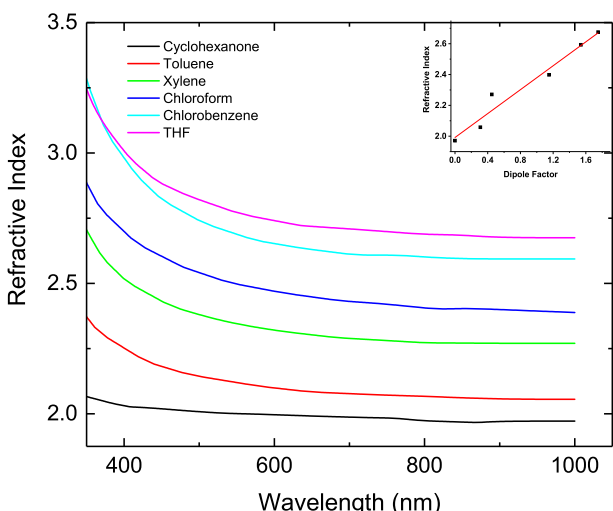


Fig. 8. Refractive index for MDMO-PPV films casted from different solvents. The dependence of refractive index on the dipole factor of solvents (inset). Scheme 1. Chemical structure of conjugated polymer MDMO-PPV.

Acknowledgement

This research project was supported by a grant from “The Research Center of the Female Scientific and Medical Colleges,” Deanship of Scientific Research, King Saud University.

References

- Alfassi, Z., Huie, R., Neta, P., Shoultz, L., 1990. Temperature dependence of the rate constants for reaction of inorganic radicals with organic reductants. *J. Phys. Chem.* 94, 8800–8805.
- Baghgar, M., Labastide, J.A., Bokel, F., Hayward, R.C., Barnes, M.D., 2014. Effect of polymer chain folding on the transition from H- to J-aggregate behavior in P3HT nanofibers. *J. Phys. Chem. C* 118, 2229–2235.
- Basko, D., Conwell, E., 2002. Hot exciton dissociation in conjugated polymers. *Phys. Rev. B* 66, 155210.
- Batchelder, J., Zewail, A., Cole, T., 1981. Luminescent solar concentrators. 2: experimental and theoretical analysis of their possible efficiencies. *Appl. Opt.* 20, 3733–3754.
- Brédas, J.-L., 1985. Relationship between band gap and bond length alternation in organic conjugated polymers. *J. Chem. Phys.* 82, 3808–3811.
- Brédas, J.L., Cornil, J., Heeger, A.J., 1996. The exciton binding energy in luminescent conjugated polymers. *Adv. Mater.* 8, 447–452.
- Brown, P.J., Sirringhaus, H., Harrison, M., Shkunov, M., Friend, R.H., 2001. Optical spectroscopy of field-induced charge in self-organized high mobility poly (3-hexylthiophene). *Phys. Rev. B* 63, 125204.
- Coakley, K.M., McGehee, M.D., 2004. Conjugated polymer photovoltaic cells. *Chem. Mater.* 16, 4533–4542.
- Debije, M.G., Verbunt, P.P., 2012. Thirty years of luminescent solar concentrator research: solar energy for the built environment. *Adv. Energy Mater.* 2, 12–35.
- Demas, J., Crosby, G.A., 1971. Measurement of photoluminescence quantum yields—Review. *J. Phys. Chem.* 75, 991.
- Dienel, T., Bauer, C., Dolamic, I., Brühwiler, D., 2010. Spectral-based analysis of thin film luminescent solar concentrators. *Sol. Energy* 84, 1366–1369.
- El-Bashir, S., 2012. Photophysical Properties of PMMA Nanohybrids and their Applications: Luminescent Solar Concentrators & Smart Greenhouses. LAP LAMBERT Academic Publishing.
- El-Bashir, S., Barakat, F., AlSalhi, M., 2014. Double layered plasmonic thin-film luminescent solar concentrators based on polycarbonate supports. *Renewable Energy* 63, 642–649.
- El-Bashir, S., Al-Harbi, F., Elburaih, H., Al-Faifi, F., Yahia, I., 2016. Red photoluminescent PMMA nanohybrid films for modifying the spectral distribution of solar radiation inside greenhouses. *Renewable Energy* 85, 928–938.
- El-Bashir, S., Alenazi, W., AlSalhi, M., 2017. Optical dispersion parameters and stability of poly (9, 9'-di-n-octylfluorenyl-2,7-diyl)/ZnO nanohybrid films: towards organic photovoltaic applications. *Mater. Res. Express* 4, 025503.
- El-Bashir, S., Yahia, I., Binhussain, M., AlSalhi, M., 2017. Designing of PVA/rose bengal long-pass optical window applications. *Results Phys.*
- El-Shaarawy, M., El-Bashir, S., Hammam, M., El-Mansy, M., 2007. Bent fluorescent solar concentrators (BFSCs): spectroscopy, stability and outdoor performance. *Curr. Appl. Phys.* 7, 643–649.
- Feng, L., Wang, F., Niu, M.-S., Zheng, F., Bi, P.-Q., Yang, X.-Y., Xu, W.-L., Hao, X.-T., 2017. Structural and optical properties of conjugated polymer and carbon-based non-fullerene material blend films for photovoltaic applications. *Opt. Mater. Express* 7, 687–697.
- Fox, M., 2002. Optical Properties of Solids. AAPT.
- Frolov, S., Gellermann, W., Ozaki, M., Yoshino, K., Vardeny, Z.V., 1997. Cooperative emission in π -conjugated polymer thin films. *Phys. Rev. Lett.* 78, 729.
- Frolov, S., Shkunov, M., Fujii, A., Yoshino, K., Vardeny, Z.V., 2000. Lasing and stimulated emission in π/π -conjugated polymers. *IEEE J. Quantum Electron.* 36, 2–11.
- Gündüz, B., 2015. Optical properties of poly [2-methoxy-5-(3', 7'-dimethoxyloxy)-1, 4-phenylenevinylene] light-emitting polymer solutions: effects of molarities and solvents. *Polym. Bull.* 72, 3241–3267.
- Gupta, R., Park, J., Srdanov, V., Heeger, A., 2002. Temperature dependence of amplified spontaneous emission in conjugated polymers. *Synth. Met.* 132, 105–107.
- Gutierrez, G.D., Coropceanu, I., Bawendi, M.G., Swager, T.M., 2016. A low reabsorbing luminescent solar concentrator employing π -conjugated polymers. *Adv. Mater.* 28, 497–501.
- Hadzioannou, G., Van Hutten, P., 2000. Semiconducting Polymers. Wiley VCH.
- Kim, J.Y., Lee, K., Coates, N.E., Moses, D., Nguyen, T.-Q., Dante, M., Heeger, A.J., 2007. Efficient tandem polymer solar cells fabricated by all-solution processing. *Science* 317, 222–225.
- Koenhen, D., Smolders, C., 1975. The determination of solubility parameters of solvents and polymers by means of correlations with other physical quantities. *J. Appl. Polym. Sci.* 19, 1163–1179.
- Krebs, F.C., 2009. Fabrication and processing of polymer solar cells: a review of printing and coating techniques. *Sol. Energy Mater. Sol. Cells* 93, 394–412.
- Lakowicz, J.R., Masters, B.R., 2008. Principles of fluorescence spectroscopy. *J. Biomed. Opt.* 13, 029901.

- Lampert, Z.E., Papanikolas, J.M., Lappi, S.E., Reynolds, C.L., 2017. Intrinsic gain and gain degradation modulated by excitation pulse width in a semiconducting conjugated polymer. *Opt. Laser Technol.* 94, 77–85.
- Lemmer, U., Heun, S., Mahrt, R., Scherf, U., Hopmeier, M., Siegner, U., Go, E., Mu, K., Ba, H., 1995. Aggregate fluorescence in conjugated polymers. *Chem. Phys. Lett.* 240, 373–378.
- Liang, Y., Xu, Z., Xia, J., Tsai, S.T., Wu, Y., Li, G., Ray, C., Yu, L., 2010. For the bright future—bulk heterojunction polymer solar cells with power conversion efficiency of 7.4%. *Adv. Mater.* 22.
- Liu, X., Ye, L., Zhao, W., Zhang, S., Li, S., Su, G.M., Wang, C., Ade, H., Hou, J., 2017. Morphology control enables thickness-insensitive efficient nonfullerene polymer solar cells. *Mater. Chem. Front.*
- Mandoc, M.M., Veurman, W., Koster, L.J.A., de Boer, B., Blom, P.W., 2007. Origin of the reduced fill factor and photocurrent in MDMO-PPV: PCNEPV all-polymer solar cells. *Adv. Funct. Mater.* 17, 2167–2173.
- Martens, T., D'Haen, J., Munters, T., Beelen, Z., Goris, L., Manca, J., D'Olieslaeger, M., Vanderzande, D., De Schepper, L., Andriessen, R., 2003. Disclosure of the nanostructure of MDMO-PPV: PCBM bulk hetero-junction organic solar cells by a combination of SPM and TEM. *Synth. Met.* 138, 243–247.
- McGehee, M.D., Heeger, A.J., 2000. Semiconducting (conjugated) polymers as materials for solid-state lasers. *Adv. Mater.* 12, 1655–1668.
- Mohan, S.R., Joshi, M., Dhami, T., Awasthi, V., Shalu, C., Singh, B., Singh, V., 2017. Charge transport in thin films of MDMO PPV dispersed with lead sulfide nanoparticles. *Synth. Met.* 224, 80–85.
- Moreno, M., Barriuso, M., Aramburu, J., 1992. The Huang-Rhys factor S (a1g) for transition-metal impurities: a microscopic insight. *J. Phys.: Condens. Matter* 4, 9481.
- Nguyen, T.-Q., Doan, V., Schwartz, B.J., 1999. Conjugated polymer aggregates in solution: control of interchain interactions. *J. Chem. Phys.* 110, 4068–4078.
- Nguyen, T.-Q., Martini, I.B., Liu, J., Schwartz, B.J., 2000. Controlling interchain interactions in conjugated polymers: the effects of chain morphology on exciton–exciton annihilation and aggregation in MEH–PPV films. *J. Phys. Chem. B* 104, 237–255.
- Nguyen, T.-Q., Schwartz, B.J., Schaller, R.D., Johnson, J.C., Lee, L.F., Haber, L.H., Saykally, R.J., 2001. Near-field scanning optical microscopy (NSOM) studies of the relationship between interchain interactions, morphology, photodamage, and energy transport in conjugated polymer films. *J. Phys. Chem. B* 105, 5153–5160.
- Oliveira, F., Cury, L., Righi, A., Moreira, R., Guimaraes, P., Matinaga, F., Pimenta, M., Nogueira, R., 2003. Temperature effects on the vibronic spectra of BEH-PPV conjugated polymer films. *J. Chem. Phys.* 119, 9777–9782.
- Österbacka, R., An, C.P., Jiang, X., Vardeny, Z.V., 2000. Two-dimensional electronic excitations in self-assembled conjugated polymer nanocrystals. *Science* 287, 839–842.
- Pankove, J.I., 2012. Optical Processes in Semiconductors. Courier Corporation.
- Park, S.H., Roy, A., Beaupré, S., Cho, S., Coates, N., Moon, J.S., Moses, D., Leclerc, M., Lee, K., Heeger, A.J., 2009. Bulk heterojunction solar cells with internal quantum efficiency approaching 100%. *Nat. Photonics* 3, 297–302.
- Quan, S., Teng, F., Xu, Z., Qian, L., Hou, Y., Wang, Y., Xu, X., 2006. Solvent and concentration effects on fluorescence emission in MEH-PPV solution. *Eur. Polym. J.* 42, 228–233.
- Rahmanudin, A., Sivula, K., 2017. Molecular strategies for morphology control in semiconducting polymers for optoelectronics. *CHIMIA Int. J. Chem.* 71, 369–375.
- Ren, S., Zhao, N., Crawford, S.C., Tambe, M., Bulović, V., Gradečak, S., 2010. Heterojunction photovoltaics using GaAs nanowires and conjugated polymers. *Nano Lett.* 11, 408–413.
- Rispens, M.T., Meetsma, A., Rittberger, R., Brabec, C.J., Sariciftci, N.S., Hummelen, J.C., 2003. Influence of the solvent on the crystal structure of PCBM and the efficiency of MDMO-PPV: PCBM ‘plastic’ solar cells. *Chem. Commun.* DOI 1, 2116–2118.
- Salleo, A., 2007. Charge transport in polymeric transistors. *Mater. Today* 10, 38–45.
- Salleo, A., Chen, T., Völkel, A., Wu, Y., Liu, P., Ong, B., Street, R., 2004. Intrinsic hole mobility and trapping in a regioregular poly (thiophene). *Phys. Rev. B* 70, 115311.
- Sirringhaus, H., Wilson, R., Friend, R., Inbasekaran, M., Wu, W., Woo, E., Grell, M., Bradley, D., 2000. Mobility enhancement in conjugated polymer field-effect transistors through chain alignment in a liquid-crystalline phase. *Appl. Phys. Lett.* 77, 406–408.
- Skotheim, T.A., 1997. Handbook of Conducting Polymers. CRC Press.
- Spano, F.C., Silva, C., 2014. H-and J-aggregate behavior in polymeric semiconductors. *Annu. Rev. Phys. Chem.* 65, 477–500.
- Sumitani, M., Nakashima, N., Yoshihara, K., Nagakura, S., 1977. Temperature dependence of fluorescence lifetimes of trans-stilbene. *Chem. Phys. Lett.* 51, 183–185.
- Swartz, B., Cole, T., Zewail, A., 1977. Photon trapping and energy transfer in multiple-dye plastic matrices: an efficient solar-energy concentrator. *Opt. Lett.* 1, 73–75.
- Tauc, J., 1970. Absorption edge and internal electric fields in amorphous semiconductors. *Mater. Res. Bull.* 5, 721–729.
- Traiphol, R., Sanguansat, P., Srikrarin, T., Kerdcharoen, T., Osotchan, T., 2006. Spectroscopic study of photophysical change in collapsed coils of conjugated polymers: effects of solvent and temperature. *Macromolecules* 39, 1165–1172.
- van Bavel, S., Veenstra, S., Loos, J., 2010. On the importance of morphology control in polymer solar cells. *Macromol. Rapid Commun.* 31, 1835–1845.
- van Hal, P.A., Wienk, M.M., Kroon, J.M., Verhees, W.J., Slooff, L.H., van Gennip, W.J., Jonkheijm, P., Janssen, R.A., 2003. Photoinduced Electron Transfer and Photovoltaic Response of a MDMO-PPV: TiO₂ Bulk-Heterojunction. *Adv. Mater.* 15, 118–121.
- Wienk, M.M., Kroon, J.M., Verhees, W.J., Knol, J., Hummelen, J.C., van Hal, P.A., Janssen, R.A., 2003. Efficient methano [70] fullerene/MDMO-PPV bulk heterojunction photovoltaic cells. *Angew. Chem.* 115, 3493–3497.
- Yao, Y., Hou, J., Xu, Z., Li, G., Yang, Y., 2008. Effects of solvent mixtures on the nanoscale phase separation in polymer solar cells. *Adv. Funct. Mater.* 18, 1783–1789.
- Zheng, T., Lu, L., Jackson, N.E., Lou, S.J., Chen, L.X., Yu, L., 2014. Roles of quinoidal character and regioregularity in determining the optoelectronic and photovoltaic properties of conjugated copolymers. *Macromolecules* 47, 6252–6259.